Tailored diffraction asymmetries from spatially odd-symmetric phase gratings

Shuo Hua,[1,2,*] Yi-Mou Liu,[1,*] G. E. Lio,[3] Xiao-Jun Zhang,[1] Jin-Hui Wu,[1,†] M. Artoni,[3,4,‡] and G. C. La Rocca[5,§]

[1]*Center for Quantum Sciences and School of Physics, Northeast Normal University, Changchun 130024, People's Republic of China*

[2]*School of Science, Jilin Institute of Chemical Technology, Jilin 132022, People's Republic of China*

[3]*Department of Physics and European Laboratory for Nonlinear Spectroscopy (LENS), University of Florence, Sesto Fiorentino, 50019 Florence, Italy*

[4]*Department of Engineering and Information Technology and Istituto Nazionale di Ottica (INO-CNR), Brescia University, 25133 Brescia, Italy*

[5]*NEST, Scuola Normale Superiore, 56126 Pisa, Italy*

(Received 29 August 2021; revised 25 March 2022; accepted 19 April 2022; published 11 May 2022)

Phase gratings, each period of which consists of even numbers of equal-width and equal-thickness *elements,* can be devised to attain asymmetric diffraction patterns. We show that engineering of offset refractive indices in different elements exhibiting a spatially odd symmetry leads to the elimination of a single diffraction order (*directional elimination*), while further manipulations on offset refractive indices may lead to the elimination of all odd or even orders (*grouped elimination*) or all orders but one or two selected (*directional selection*). These intriguing effects arise from destructive interference between diffracted amplitudes contributed by paired or successive elements, and violation of Friedel's law in such transparent gratings is an effect of higher order multiple scattering.

DOI: 10.1103/PhysRevResearch.4.023113

I. INTRODUCTION

Diffraction gratings, discovered at least three centuries ago, are crucial components of instruments that have enabled important developments in many fields of science and technology, including physics, astronomy, chemistry, and biology [1–4]. Underlying principles of light diffraction, on the other hand, have always been an intriguing subject from a fundamental point of view ever since Grimaldi's first characterization and Young's celebrated experiment on this effect. The latter, e.g., helped in understanding that light must propagate as a wave supporting Huygens' original wave theory of light [5]. A traditional (etched) grating, consisting of a periodic binary structure made from nonabsorbing and amplifying materials, has somewhat limited applications due to the fact that its diffraction pattern is (I) *fixed* and (II) *symmetric* about the incident direction, however.

Over the past two decades, reconfigurable gratings to overcome the disadvantage that diffraction patterns cannot be modulated (I) have been proposed and realized. Electromagnetically induced gratings (EIGs) [6–9] are probably the most familiar ones and have attracted great interest because they are readily controlled while bearing broad application prospects. Approaches based, e.g., on microwave composite phase modulation and Kerr enhanced cross-phase modulation were also proposed to improve the grating performance [10–15]. Overcoming the symmetry disadvantage (II) may be more demanding in applications. As a matter of fact, diffraction from a crystal is expected to be symmetric even if the crystal has no center of inversion. This is known as Friedel's law [16] that holds when (a) scattering is *weak*, in the sense that only first-order processes are relevant, and when (b) there is no *absorption*. To be more specific, the diffraction intensity $I(\vec{G})$ corresponding to a wave-vector change $\vec{G}$ is proportional to the modulus square of the Fourier component $V(\vec{G})$ of a scattering potential, and hence Friedel's law $I(\vec{G}) = I(-\vec{G})$ follows when we have $V(-\vec{G}) = V^*(\vec{G})$ for a real potential. In the case of x-ray scattering, where Friedel's law was originally formulated, requirement (a) means that the kinematic diffraction theory, as opposed to the general dynamical diffraction theory, works while requirement (b) means that the polarizability is real [17]. Clearly, Friedel's law can be generalized to diffractions of electrons, neutrons, and atoms, provided scattering processes arise from a weak and real potential.

The realization and control of diffraction asymmetries are very important, e.g., in modern light-wave communications though it is obviously a more difficult task. In the case of x-ray scattering, mild violations of Friedel's law are commonly found because of absorption, see point (b) above, as predicted by Ewald *et al.* [18] and observed in zincblende crystals [19]. The underlying physics lies in the spatial phase shift of a refractive-index (phase) grating relative to an absorption (amplitude) grating. That means, complex scattering potentials were used whereby an out-of-phase modulation of phases and amplitudes of the scattered waves gives rise to diffraction asymmetries [20,21]. Strongly asymmetric patterns have been

*These authors contributed equally to this work.
†jhwu@nenu.edu.cn
‡maurizio.artoni@unibs.it
§g.larocca@sns.it

achieved with atomic beams diffracted by a tailored complex potential (optical lattice) [20]. In optics, such out-of-phase modulations are also called non-Hermitian modulations, and parity-time ($\mathcal{PT}$) symmetric modulations are attained in particular when the refractive index is an even function while the absorption is an odd function in space. So far, quite a few examples of one-dimension and two-dimension asymmetric diffractive gratings based on $\mathcal{PT}$ symmetric or more general non-Hermitian modulations have recently been proposed [22–29].

While non-Hermitian gratings are effective to achieve asymmetric diffraction, they hinge, however, on an accurate control on spatial distributions of both absorption-gain and refractive index. Then a question arises of whether it is viable to break Friedel's law so as to realize, and more importantly tailor on demand, diffraction asymmetries in a phase grating by modulating the spatial distribution of only refractive index. The answer is positive when scattering processes can no longer be considered weak; see point (a) above. The possibility of observing diffraction asymmetries solely due to higher order scattering, originally brought forward many decades ago [30,31] for electrons, has recently been demonstrated also in two-dimension materials [32]. Needless to say, the search for asymmetric diffraction due to a breakdown of the weak scattering requirement in Friedel's law is rather elusive in the optical regime. Yet, we reckon it would be important not only for real applications but also from a more fundamental point of view. This is relevant to binary optics as far as light diffraction is concerned, which allows one to make micron-level (relief) phase elements based on computer-aided designs for realizing various wave filtering functions like angle selection, color separation, and rotational asymmetry [33–38]. A more flexible and complete control of the flow of light is now viable via metasurfaces—planar and ultrathin metamaterials composed of subwavelength building blocks—as an effective extension of binary optical devices [39–44].

Here we explain how to engineer a pure phase grating in the spirit of extended binary optics that can lead to asymmetric diffraction in the presence of multiple scattering processes. *First*, we provide a theoretical framework to tackle diffraction asymmetries by introducing a multielement periodic structure into our phase grating. Results for light intensities corresponding to different diffraction orders show that asymmetric higher order scattering occurs when offset refractive indices of different elements exhibit a spatially odd symmetry. *Second*, we provide an elaborate procedure to derive specific conditions under which diffraction patterns can be tailored by suppressing one or more selected diffraction orders. Three examples of diffraction asymmetries are discussed and shown via numerical calculations, namely directional elimination of a single diffraction order, grouped elimination of all even or odd diffraction orders, and directional selection of one or two diffraction orders.

II. MODEL AND EQUATIONS

We start by considering a one-dimension phase grating of period a along the x direction, which will result in the diffraction of a light beam incident along the z direction into a few symmetric orders $j \in \{-J, J\}$ as shown in Fig. 1(a). Each

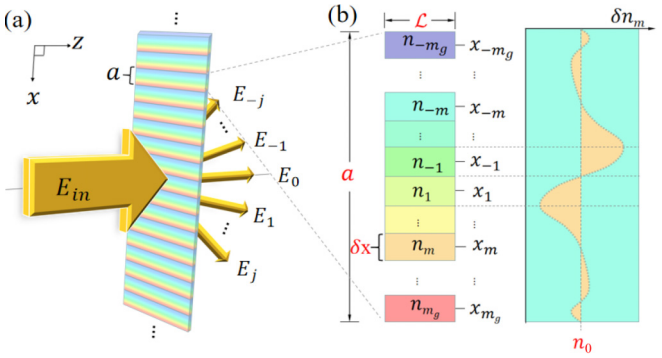

FIG. 1. (a) Schematic of a phase grating of period a along the x direction, which can diffract a light beam of amplitude E_{in} incident along the z direction into a few light beams of amplitudes E_j deviating with angles θ_j relative to the z direction. (b) Fine structure in a period consisting of $2m_g$ elements with a common width $\delta x = a/2m_g$ and a common thickness $\mathcal{L}$ while different refractive indices $n_m = n_0 + \delta n_m$, e.g., restricted by $\delta n_m = -\delta n_{-m}$ in the limit of $m_g \to \infty$.

period is designed to have $2m_g$ elements with an identical width $\delta x = a/2m_g$ along the x direction but different refractive indices $n_m = n_0 + \delta n_m$ for $|m| \in \{1, m_g\}$, with n_0 being the mean value while δn_m denoting the offset values, as shown in Fig. 1(b). In order to have an asymmetric diffraction pattern, we must take $m_g > 1$ because a centrosymmetric unit cell can always be chosen in the binary case ($m_g = 1$). Taking $\mathcal{L}$ as the common thickness for all elements and considering a probe field with wavelength λ_p and wave vector $k_p = 2\pi/\lambda_p$, we can write down the individual transmission function

$$T_m = e^{in_m k_p \mathcal{L}} = e^{i\delta n_m k_p \mathcal{L}}, \tag{1}$$

of the mth element, where the immaterial common phase factor $e^{in_0 k_p \mathcal{L}}$ has been removed for simplicity. Each period of this multielement phase grating can be described by the total transmission function

$$T(x) = \sum_{m=-m_g}^{m_g} T_m \text{rect}\left(\frac{x - x_m}{\delta x}\right), \tag{2}$$

being $x_m = (2m+1)a/4m_g$ for $m \leqslant -1$ while $x_m = (2m-1)a/4m_g$ for $m \geqslant 1$ the mth element's center. Note that the term $m = 0$ is not present in the summation above and the following ones. It is also worth noting that $T(x)$ in Eq. (2) for a finite grating thickness $\mathcal{L}$ is valid only if resonator effects are negligible between different elements and at grating boundaries. This approximation of geometrical optics can be justified by choosing $n_0 \gg |\delta n_m|$ and $a \gg \lambda_p$ to avoid significant reflections by simultaneously reducing reflectivities and diffraction angles, as supported by previous works on EIGs realized with cold atoms [7–11] where periodic changes of refractive indices are induced by standing-wave laser fields.

Further considering the translational invariance, we now make a Fourier transform to expand the total transmission function into $T(x) = \int_{-k_p}^{k_p} E(\theta) e^{ik_x x} dk_x$, where θ refers to an angle deviating from the z direction in the xz plane while $k_x = k_p \sin\theta$ denotes a projection of k_p from the direction determined by angle θ to the x direction. An inverse procedure of

this Fourier transform then yields the dimensionless amplitude

$$E(\theta) = \frac{2\sin(k_x \delta x/2)}{a k_x} \sum_{m=-m_g}^{m_g} e^{i(\delta n_m k_p \mathcal{L} - k_x x_m)}, \tag{3}$$

for a normally incident light beam diffracted into angle θ. It is thus straightforward to write down the diffraction intensity contributed by M irradiated periods

$$I(\theta) = |E(\theta)|^2 \frac{\sin^2(\pi M R \sin\theta)}{M^2 \sin^2(\pi R \sin\theta)}, \tag{4}$$

where the beam width W_b has been taken into account in terms of the ratio $M = W_b/a$.

Diffraction peaks are known to occur at discrete angles θ_j determined by $k_j = k_p \sin\theta_j = j2\pi/a$ or $j = R\sin\theta_j$ with $R = a/\lambda_p$. Based on this consideration, we would pay special attention to the jth-order diffraction by examining $E_j = E(\theta_j)$ for $j \neq 0$. Setting $\alpha_m = \delta n_m k_p \mathcal{L}$, $\beta_m^j = k_j x_m$, and $A_j = \sin(j\pi/2m_g)/j\pi$, we can make a power series expansion of Eq. (3) to attain

$$E_j = \sum_{m=-m_g}^{m_g} A_j e^{-i\beta_m^j} \left[i\alpha_m - \frac{\alpha_m^2}{2} - \frac{i\alpha_m^3}{6} + \cdots \right]. \tag{5}$$

Defining $g_{jr} = \sum A_j \cos\beta_m^j \alpha_m$, $g_{ji} = \sum A_j \sin\beta_m^j \alpha_m$, $h_{jr} = \sum A_j \cos\beta_m^j \alpha_m^2$, and $h_{ji} = \sum A_j \sin\beta_m^j \alpha_m^2$, with the replacement $\alpha_m \to \varepsilon_j \alpha_m$, we further have

$$E_j \approx \left(g_{ji}\varepsilon_j - h_{jr}\varepsilon_j^2/2\right) + i\left(g_{jr}\varepsilon_j + h_{ji}\varepsilon_j^2/2\right), \tag{6}$$

where factor ε_j is so small that it is enough to keep only the first- and second-order scattering terms. Considering $g_{jr} = g_{-jr}$, $g_{ji} = -g_{-ji}$, $h_{jr} = h_{-jr}$, and $h_{ji} = -h_{-ji}$, it is then viable to write down intensities

$$I_{\pm j} \approx \left|g_{ji}\varepsilon_j \mp h_{jr}\varepsilon_j^2/2\right|^2 + \left|g_{jr}\varepsilon_j \pm h_{ji}\varepsilon_j^2/2\right|^2 \tag{7}$$

for the $\pm j$th diffraction orders. Accordingly, we can introduce the intensity contrast ratio

$$C_j = \frac{I_j - I_{-j}}{I_j + I_{-j}} \approx \frac{g_{jr}h_{ji} - g_{ji}h_{jr}}{g_{jr}^2 + g_{ji}^2}\varepsilon_j \tag{8}$$

to evaluate the degree of diffraction asymmetries. Considering $\beta_{-m}^j = -\beta_m^j$ and $\alpha_m = \delta n_m k_p \mathcal{L}$, it is not difficult to find $g_{jr}h_{ji} = g_{ji}h_{jr}$ in the case of $\delta n_{-m} = \delta n_m$ (spatially even symmetry) while $g_{jr}h_{ji} = -g_{ji}h_{jr}$ in the case of $\delta n_{-m} = -\delta n_m$ (spatially odd symmetry). Thus, higher order scattering processes will lead to diffraction asymmetries as long as δn_m is not of spatially even symmetry, and largest asymmetries definitely occur when δn_m exhibits a spatially odd symmetry.

In what follows, we restrict our discussions to diffraction peaks with $k_x = k_j$ only in the case of $\delta n_m = -\delta n_{-m}$ such that Eq. (3) can be translated into

$$E_j = \frac{\sin(j\pi/2m_g)}{j\pi/2} \sum_{m=1}^{m_g} \cos\left(\alpha_m - \beta_m^j\right) \tag{9}$$

for the jth diffraction order. From this equation, it is not difficult to see that we can attain $E_j = 0$ by requiring $\alpha_m^j = \beta_m^j + (l_m^j - 1/2)\pi$, being l_m^j an integer. In this case, transmitted light beams out of the $\pm m$th elements will exhibit opposite phase shifts $\pm(l_m^j - 1/2)\pi$ and thus have a vanishing contribution to the jth diffraction order due to a paired destructive interference. Such a requirement on l_m^j can be satisfied by engineering offset refractive indices $\delta n_m^j = -\delta n_{-m}^j$ according to

$$\delta n_m^j = \frac{\left[j(2m-1) + \left(2l_m^j - 1\right)m_g\right]\lambda_p}{4m_g\mathcal{L}}, \tag{10}$$

where l_m^j can be chosen at will for each value of $m \in \{1, m_g\}$ to realize the *directional elimination* of a single diffraction peak of any order $j \in \{-J, J\}$.

We then consider whether it is possible to further have $E_{j\pm 2k} = 0$ with $k \in \{1, 2, 3, \ldots\}$ on the basis of $E_j = 0$, realizing thus the *grouped elimination* of all even or odd diffraction orders. To this end, we note that

$$E_{j\pm 2k} = \frac{\sin[(j \pm 2k)\pi/2m_g]}{(j \pm 2k)\pi/2} \sum_{m=1}^{m_g} \sin\left(l_m^j\pi \mp k\delta_m\right), \tag{11}$$

with $\delta_m = (2m-1)\pi/m_g$ being the mean phase shift of the $(j-2)$th diffraction order relative to the jth diffraction order contributed by the $\pm m$th elements. Accordingly, $E_{j\pm 2k}$ will become vanishing if we require

$$\sin\left(l_m^j\pi \mp k\delta_m\right) + \sin\left(l_{m^*}^j\pi \mp k\delta_{m^*}\right) = 2\sin\left[\frac{\left(l_m^j + l_{m^*}^j\right)}{2}\pi \mp k\pi\right]\cos\left[\frac{\left(l_m^j - l_{m^*}^j\right)}{2}\pi \mp \frac{k(m-m^*)}{m_g}\pi\right] = 0, \tag{12}$$

with $m^* = m_g - m + 1$ denoting the conjugate element of the mth element. Note, however, that

$$\sin\left(l_{m_{g/2}}^j\pi \mp k\delta_{m_{g/2}}\right) = \sin\left(l_{m_{g/2}}^j\pi \mp k\pi\right) = 0, \tag{13}$$

where $m_{g/2} = m_{g/2}^* \equiv (m_g + 1)/2$ is also required if m_g is an odd integer. It is thus clear that all even or odd diffraction orders will disappear when (*i*) j is an even or odd integer and (*ii*) $l_m^j + l_{m^*}^j$ is chosen as an even integer to ensure $\sin[(l_m^j + l_{m^*}^j)\pi/2] = 0$. This can be easily understood by reiterating the discussion above Eq. (10) except that a dual paired destructive interference occurs as the $\sin(l_m^j\pi \mp k\delta_m)$ terms of $\pm m$th elements cancel the $\sin(l_{m^*}^j\pi \mp k\delta_{m^*})$ terms of $\pm m^*$th elements. The extra requirement on $l_m^j + l_{m^*}^j$ can also be satisfied by engineering offset refractive indices $\delta n_m^j = -\delta n_{-m}^j$ according to Eq. (10). Other diffraction orders $E_{j\pm(2k-1)}$ are nonzero, however, because Eqs. (12) and (13) do not hold again with the replacement $k\pi \to (k - 1/2)\pi$.

TABLE I. Sufficient conditions for realizing three types of asymmetric diffraction patterns.

Directional elimination	Grouped elimination	Directional selection
$l_m^j = 0, \pm 1, \pm 2, \pm 3, \ldots$	$l_m^j + l_{m^*}^j = 0, \pm 2, \pm 4, \pm 6, \ldots$	$l_{m+1}^j - l_m^j = \pm 1, \pm 3, \pm 5, \ldots$
$\delta n_m^j = -\delta n_{-m}^j$	$\delta n_m^j = -\delta n_{-m}^j$	$\delta n_m^j = -\delta n_{-m}^j$
$\delta n_m^j = \frac{[j(2m-1)+(2l_m^j-1)m_g]\lambda_p}{4m_g\mathcal{L}}$	$\delta n_m^j = \frac{[j(2m-1)+(2l_m^j-1)m_g]\lambda_p}{4m_g\mathcal{L}}$	$\delta n_m^j = \frac{[j(2m-1)+(2l_m^j-1)m_g]\lambda_p}{4m_g\mathcal{L}}$

Finally, we consider whether it is possible to realize a more interesting case of $E_{j\pm k} = 0$ except for a specific value of $k \in \{1, 2, 3, \ldots\}$ on the basis of $E_j = 0$, realizing thus the *directional selection* of a single diffraction order on demand. To this end, we note that

$$E_{j\pm k} = \frac{\sin[(j \pm k)\pi/2m_g]}{(j \pm k)\pi/2} \sum_{m=1}^{m_g} \sin\left(l_m^j\pi \mp \frac{k\delta_m}{2}\right), \quad (14)$$

which will become vanishing if we require

$$\sum_{m=1}^{m_g} \cos\left(\frac{k\delta_1}{2}\right) \sin\left(l_m^j\pi \mp \frac{k\delta_m}{2}\right) = \frac{1}{2}\sum_{m=1}^{m_g} \sin\left(l_m^j\pi \mp \frac{km}{m_g}\pi \pm \frac{k}{m_g}\pi\right) + \sin\left(l_m^j\pi \mp \frac{km}{m_g}\pi\right) = 0, \quad (15)$$

in the case of $k \neq \widetilde{m}_g \in \{1, 3, 5, \ldots\}m_g$ so as to guarantee $\cos(k\delta_1/2) = \cos(k\pi/2m_g) \neq 0$. Defining $l_{m_g+1}^j \equiv l_1^j \pm k$, we can further translate this equation into

$$\sum_{m=1}^{m_g} \sin\left(\frac{l_m^j + l_{m+1}^j}{2}\pi \mp \frac{km}{m_g}\pi\right) \cos\left(\frac{l_{m+1}^j - l_m^j}{2}\pi\right) = 0, \quad (16)$$

after a *sequential summation* of the $2m_g$ sine functions. It is thus clear that we can attain $E_{j\pm k} = 0$ for $k \neq \widetilde{m}_g$ as long as $l_{m+1}^j - l_m^j$ is chosen as an odd integer to ensure $\cos[(l_{m+1}^j - l_m^j)\pi/2] = 0$. This can be easily understood by reiterating the discussion above Eq. (10) except that a successive paired destructive interference occurs as the $\sin[l_m^j \mp km/m_g]\pi$ and $\sin[l_m^j \mp k(m-1)/m_g]\pi$ terms of $\pm m$th elements cancel the $\sin[l_{m+1}^j \mp km/m_g]\pi$ terms of $\pm(m+1)$th elements and the $\sin[l_{m-1}^j \mp k(m-1)/m_g]\pi$ terms of $\pm(m-1)$th elements, respectively. The extra requirement on $l_{m+1}^j - l_m^j$ can also be satisfied by engineering offset refractive indices $\delta n_m^j = -\delta n_{-m}^j$ according to Eq. (10). In the case of $k = \widetilde{m}_g$, however, a straightforward calculation from Eq. (14) yields

$$E_{j\pm\widetilde{m}_g} = \frac{\cos(j\pi/2m_g)}{(j \pm \widetilde{m}_g)\pi/2} \sum_{m=1}^{m_g} \cos\left[\left(l_m^j \mp \frac{\widetilde{m}_g}{m_g}m\right)\pi\right], \quad (17)$$

which cannot be zero because all terms in the summation are equal when $l_{m+1}^j - l_m^j$ is an odd integer. As a result, we can select a single diffraction order while eliminating all others only if just a specific value of $j \pm \widetilde{m}_g$ falls within $\{-J, J\}$, depending critically on $R = a/\lambda_p$.

Sufficient conditions derived above for realizing the directional elimination of a single diffraction order, grouped elimination of all even or odd diffraction orders, and directional selection of a few diffraction orders are summarized in Table I in terms of δn_m^j (l_m^j).

III. RESULTS AND DISCUSSION

More direct insights onto analytical results derived in the last section can be gained via numerical calculations and qualitative discussions for a phase grating reconfigurable via $\delta n_m^j = -\delta n_{-m}^j$. Our calculations and discussions will be restricted to the case of $m_g = 5$, $\mathcal{L} = 5\lambda_p$, $R = 50$, and $|\delta n_m^j| \ll n_0$ with a surrounding medium of refractive index $n \equiv n_0$. This choice is considered to restrict the maximal diffraction angle down to $\theta_{\max} \lesssim 10^o$ corresponding to $J = [R\sin\theta_{\max}] \lesssim 8$ and suppress the maximal reflectivity down to $r_{\max} \lesssim 0.25\%$ between different elements and at grating boundaries so as to justify the applicability of $T(x)$ in Eq. (2). The validity of this analytical approach has been also verified by a numerical Comsol calculation as discussed below.

A. Directional diffraction elimination

First, we verify via numerical calculations that it is viable to eliminate a desired diffraction order with appropriate values of δn_m^j according to the left column in Table I. This column tells that $\delta n_m^j = -\delta n_{-m}^j$ can be designed on demand to satisfy Eq. (10) for different combinations of j and l_m^j while m, m_g, and $\mathcal{L}/\lambda_p$ are fixed parameters. For instance, we can take $j = 1, 2$ with $l_{1,2,3,4,5}^{1,2} \equiv 0, 0, 0, -1, -1$ to eliminate the first and second diffraction orders while $j = 3, 4$ with $l_{1,2,3,4,5}^{3,4} \equiv 0, 0, -2, -1, -3$ to eliminate the third and fourth diffraction orders, respectively. Corresponding diffraction patterns are shown in Figs. 2(a_1)–2(a_4) accompanied by respective offset refractive indices in Figs. 2(b_1)–2(b_4), along with a numerical check of the validity of Eq. (2) via Comsol in Figs. 2(c_1)–2(c_3). It is clear that surviving diffraction orders are highly asymmetric and the strongest diffraction always occurs for $j' = j \pm 2$ or $j' = j \pm 2 \mp 2m_g$. Other choices of integers $l_{1,2,3,4,5}^j$ can also be used to eliminate the jth diffraction order, but may result in different diffraction asymmetries.

The underlying physics may be attributed to the destructive interference between each pair of light beams scattered by the

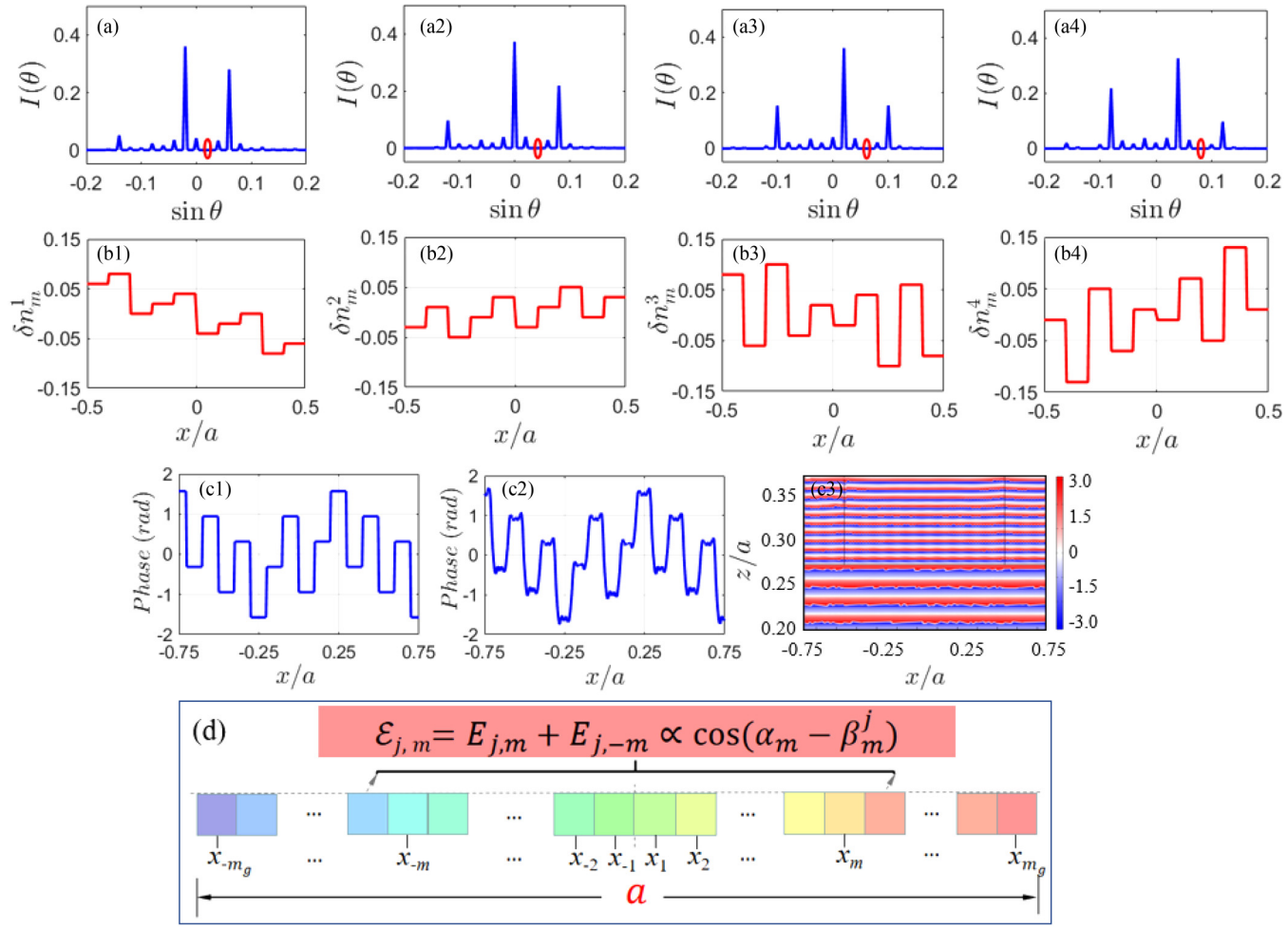

FIG. 2. Intensity I against $\sin\theta$ with a missing first (a_1), second (a_2), third (a_3), or fourth (a_4) diffraction order, and corresponding offset refractive indices δn_m^1 (b_1), δn_m^2 (b_2), δn_m^3 (b_3), or δn_m^4 (b_4) for the $2m_g$ elements in a period. (c) Comparison of the phase of $T(x)$ associated with the offset refractive indices δn_m^2 shown in (b_2) as obtained analytically from Eq. (2) (c_1) and numerically via Comsol (c_2) at the sample exit face, with the full Comsol numerical calculation shown in (c_3) . (d) Schematic of a paired destructive interference between diffracted amplitudes contributed by the $\pm m$th elements. Relevant parameters are $\lambda_p = 0.8\ \mu$m, $m_g = 5$, $R = 50$, $M = 10$, $\mathcal{L} = 5\lambda_p$, $n_0 = 2.0$, $l_{1,2,3,4,5}^{1,2} = 0, 0, 0, -1, -1$, and $l_{1,2,3,4,5}^{3,4} = 0, 0, -2, -1, -3$.

$\pm m$th elements in the same period as illustrated in Fig. 2(d). This paired destructive interference can be understood as described below. (i) We note from Eq. (3) that the jth-order light beam scattered by the mth element acquires an exact forward phase $\alpha_m = \delta n_m k_p \mathcal{L}$ and a mean deflected phase $-\beta_m^j = -k_j x_m$ in addition to a common amplitude independent of m. (ii) We write down $E_{j,\pm m} \propto e^{\pm i(\alpha_m - \beta_m^j)}$ for the $\pm m$th elements by further considering $\delta n_m = -\delta n_{-m}$ and $x_m = -x_{-m}$. (iii) We find that the $\pm m$th elements contribute a beam superposition, to the jth-order diffraction, of amplitude $\mathcal{E}_{j,m} = E_{j,m} + E_{j,-m} \propto \cos(\alpha_m - \beta_m^j)$, which will become vanishing in the case of $\alpha_m^j = \beta_m^j + (l_m^j - 1/2)\pi$. Consequently, we would observe the overall effect of jth-order directional elimination with $I(\theta_j) = 0$ as all m_g pairs of elements are made to satisfy Eq. (10).

Then we try to verify that diffraction asymmetries observed in Fig. 2 are a result of multiple higher order scattering as explained via Eq. (7) and Eq. (8). This can be done by calculating the intensity contrast ratio C_j as a function of ε_j, quantifying the strength of the phase contrast for four eliminated diffraction orders. As shown in Fig. 3, C_j vanishes linearly for all diffraction orders as ε_j is decreased in the weak scattering regime ($\varepsilon_j < 0.2$ for the parameters used here) while the maximum contrast $|C_j| \to 1$ is attained with $\varepsilon_j \approx 1$. Further increasing ε_j, we find that $|C_j|$ becomes smaller at different rates and cannot be vanishing at the same time for different diffraction orders, indicating that diffraction is in general asymmetric as long as scattering is not weak.

B. Grouped diffraction elimination

Second, we verify via numerical calculations that it is viable to eliminate all even or odd diffraction orders with appropriate values of δn_m^j according to the middle column in Table I. This column tells that the requirement $\delta n_m^j = -\delta n_{-m}^j$ should be imposed by an extra restriction $l_m^j + l_{m^*}^j = 0, \pm 2, \pm 4, \ldots$. Taking $j = 1$ and $l_{1,2,3,4,5}^1 = 0, 0, 0, 0, 0$ for instance, we can see from Fig. 4(a_1) that all odd diffraction orders are eliminated with corresponding offset refractive

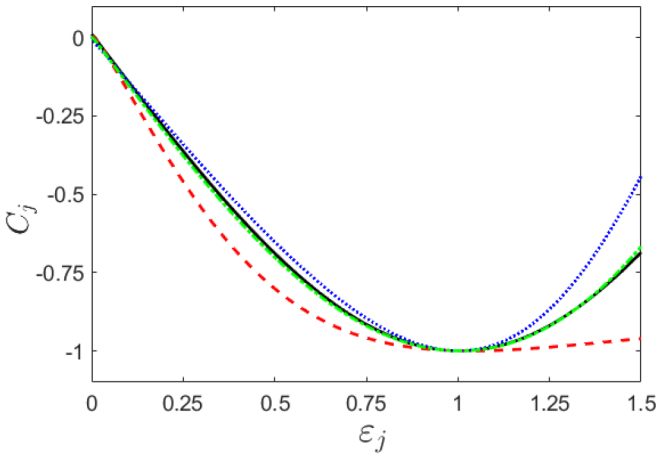

FIG. 3. Intensity contrast C_j against scattering factor ε_j. The black solid, red dashed, blue dotted, and green dash-dotted curves correspond to C_1 attained with parameters used in Fig. 2(a_1), C_2 attained with parameters used in Fig. 2(a_2), C_3 attained with parameters used in Fig. 2(a_3), and C_4 attained with parameters used in Fig. 2(a_4), respectively.

indices shown in Fig. 4(b_1). In another case of $j = 2$ and $l^2_{1,2,3,4,5} = 0, 0, 0, 0, -2$, we find from Fig. 4($a_2$) that all even diffraction orders are eliminated with corresponding offset refractive indices shown in Fig. 4(b_2). It is clear that surviving diffraction orders are highly asymmetric and $j' = j \pm 1$ refer to the two strongest diffraction orders. Other choices

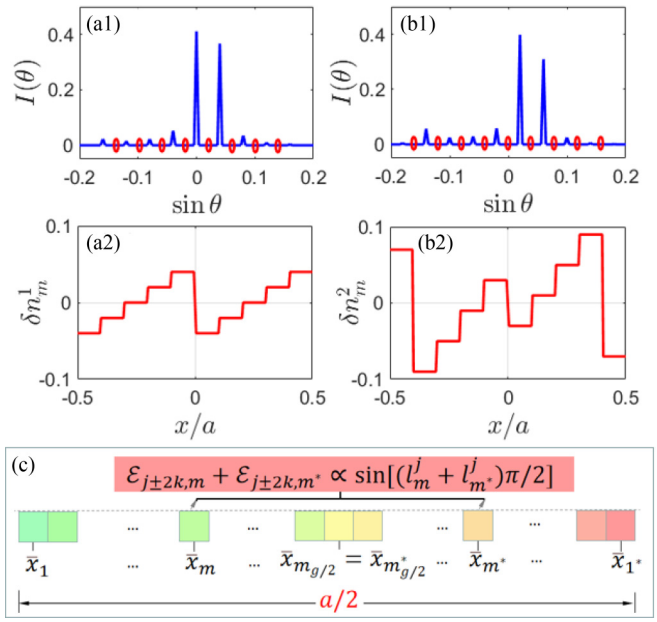

FIG. 4. Intensity I against $\sin\theta$ with all odd (a_1) or even (a_2) diffraction orders eliminated on the basis of a missing first (a_1) or second (a_2) diffraction order, and corresponding offset refractive indices δn^1_m (b_1) or δn^2_m (b_2) for the $2m_g$ elements in a period. (c) Schematic of a dual paired destructive interference between diffracted amplitudes contributed by the $\overline{m}$th and $\overline{m^*}$th elements, with $\overline{m}$ denoting a joint contribution of the $\pm m$ elements. Parameters are the same as in Fig. 2 except $l^1_{1,2,3,4,5} = 0, 0, 0, 0, 0$ and $l^2_{1,2,3,4,5} = 0, 0, 0, 0, -2$.

of $l^j_m + l^j_{m^*} = 0, \pm2, \pm4, \ldots$ can also be used to eliminate all odd or even diffraction orders, but may result in different diffraction asymmetries.

The $(j \pm 2k)$th-order diffraction elimination should be attributed to a dual paired destructive interference as illustrated in Fig. 4(c), which can also be understood in three steps. (i) We note that $\alpha^j_m - \beta^j_m = (l^j_m - 1/2)\pi$ has been taken to eliminate the jth-order diffraction, yielding thus δn^j_m in Eq. (8). (ii) On this basis, we write down $\mathcal{E}_{j\pm2k,m} \propto \sin(l^j_m\pi \mp k\delta_m)$ for the $\pm m$th elements and $\mathcal{E}_{j\pm2k,m^*} \propto \sin(l^j_{m^*}\pi \mp k\delta_{m^*})$ for the $\pm m^*$th elements by considering $\alpha^{j\pm2k}_m = \alpha^j_m$ and $\beta^{j\pm2k}_m = \beta^j_m \pm k\delta_m$. (iii) With $\delta_m + \delta_{m^*} = 2\pi$, it is easy to find that the $\pm m$th and $\pm m^*$th elements contribute a beam superposition, to the $(j \pm 2k)$th-order diffraction, of amplitude $\mathcal{E}_{j\pm2k,m} + \mathcal{E}_{j\pm2k,m^*} \propto \sin[(l^j_m + l^j_{m^*})\pi/2]$. Consequently, the $(j \pm 2k)$th diffraction orders will disappear due to a dual paired destructive interference of the conjugate $\pm m$th and $\pm m^*$th elements when $l^j_m + l^j_{m^*}$ is an even integer (l^j_m and $l^j_{m^*}$ are of the same parity).

C. Directional diffraction selection

Finally, we verify via numerical calculations that it is viable to select one or two desired diffraction orders with appropriate values of δn^j_m according to the right column in Table I. This column tells that the requirement $\delta n^j_m = -\delta n^j_{-m}$ should be imposed by an extra restriction $l^{j+1}_m - l^j_m = \pm1, \pm3, \pm5, \ldots$. Taking $j = 1$ and $l^1_{1,2,3,4,5} = 0, 1, 0, -1, 0$ for instance, we can see from Fig. 5(a_1) that the -4th and sixth diffraction orders survive due to $j' = j - m_g > -J$ and $j' = j + m_g < J$, respectively, with corresponding offset refractive indices shown in Fig. 5(b_1). In another case of $j = -4$ and $l^{-4}_{1,2,3,4,5} = 0, 1, 2, 3, 4$, we find from Fig. 5($a_2$) that the first diffraction order survives due to $j' = j + m_g < J$, while the -9th diffraction order missing due to $j' = j - m_g < -J$, with corresponding offset refractive indices shown in Fig. 5(b_2). It is clear that the first diffraction order in Fig. 5(a_2) is stronger than the -4th and sixth diffraction orders in Fig. 5(a_1) because the former spreads over in a smaller range of angle θ than the latter, though exhibiting similar spatial widths in terms of $\sin\theta$.

The $(j \pm k)$th-order diffraction elimination arises instead from a sequential destructive interference as illustrated in Fig. 5(c), which will be explained once again in three steps. (i) We note that $\alpha^j_m - \beta^j_m = (l^j_m - 1/2)\pi$ has been taken to eliminate the jth-order diffraction, yielding δn^j_m in Eq. (10). (ii) On this basis, we then write down $\mathcal{E}_{j\pm k,m} \propto \sin(l^j_m\pi \mp k\delta_m/2)$ for the $\pm m$th elements, which upon the multiplication of a nonvanishing $\cos(k\delta_1/2)$ with $k \neq \pm\widetilde{m}_g$ can be rewritten as a sum of inward $\mathcal{E}^{\text{in}}_{j\pm k,m} \propto \sin[l^j_m\pi \mp k(m-1)\pi/m_g]$ and outward $\mathcal{E}^{\text{out}}_{j\pm k,m} \propto \sin(l^j_m\pi \mp km\pi/m_g)$ components. (iii) We find that the sum of $\mathcal{E}^{\text{out}}_{j\pm k,m} + \mathcal{E}^{\text{in}}_{j\pm k,m+1}$ contributed by the $\pm m$th and $\pm(m+1)$th elements is proportional to $\cos[(l^j_{m+1} - l^j_m)\pi/2]$. Consequently, only the diffraction peaks of orders $(j \pm \widetilde{m}_g) \in \{-J, J\}$ can survive due to a sequential destructive interference of the adjacent $\pm(m+1)$th and $\pm m$th elements when $l^j_{m+1} - l^j_m$ is an odd integer (l^j_{m+1} and l^j_m are of opposite parities).

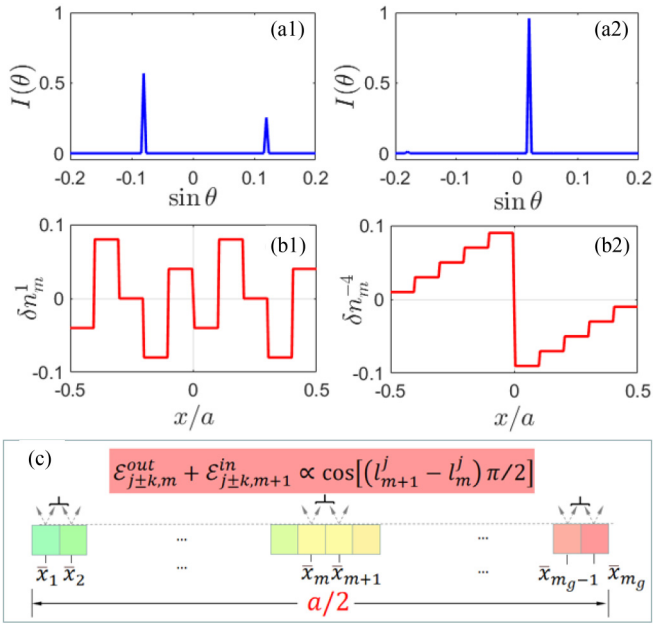

FIG. 5. Intensity I against $\sin\theta$ with a selected -4th (a_1) or first (a_2) diffraction order on the basis of a missing first (a_1) or -4th (a_2) diffraction order, and corresponding offset refractive indices δn_m^1 (b_1) or δn_m^{-4} (b_2) for the $2m_g$ elements in a period. (c) Schematic of a sequential destructive interference between diffracted amplitudes contributed by the $\overline{m}$th and $\overline{m\pm1}$th elements, with $\overline{m}$ denoting a joint contribution of the $\pm m$ elements. Parameters are the same as in Fig. 2 except $l^1_{1,2,3,4,5} = 0, 1, 0, -1, 0$ and $l^{-4}_{1,2,3,4,5} = 0, 1, 2, 3, 4$.

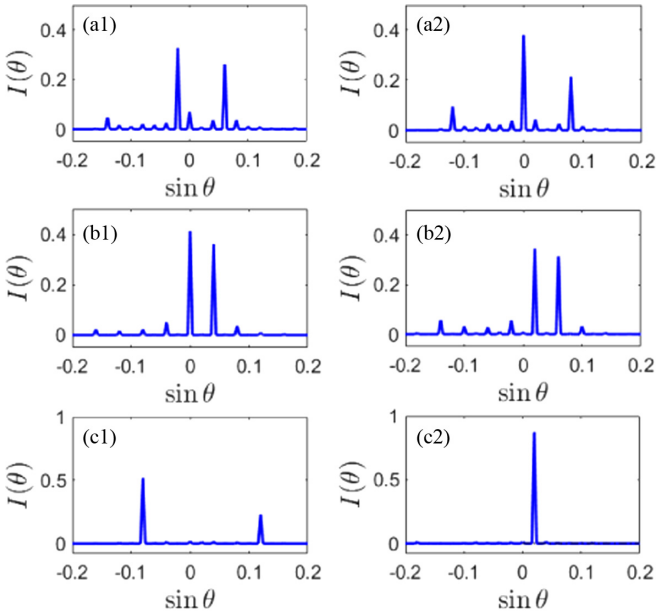

FIG. 6. Intensity I against $\sin\theta$ in the presence of disorders $r_m n_m$, with r_m being in the range of $\{-0.3, 0.3\}$. Other parameters are the same as in Figs. 2(a_1) and 2(a_2) for panels (a_1) and (a_2); as in Figs. 4(a_1) and 4(a_2) for panels (b_1) and (b_2); and as in Figs. 5(a_1) and 5(a_2) for panels (c_1) and (c_2). Each curve is attained as an average of 10 random realizations.

It is also worth noting from Eq. (17) that all selected diffraction peaks, if existent, are equally spaced with the same order difference $2m_g$. This fact indicates that we can observe a broad background with no diffraction peaks or one selected diffraction order in the case of $m_g \geqslant J$ (i), one or two selected diffraction orders in the case of $J > m_g \geqslant J/2$ (ii), and two or three selected diffraction orders in the case of $J/2 > m_g \geqslant J/3$ (iii), depending on which diffraction order is first eliminated with Eq. (10). Case (ii) has been examined above while cases (i) and (iii) may be realized by taking $m_g = 10$ and $m_g = 3$, respectively, without changing other parameters.

Finally, we assess how disorders may affect the performance of our grating due to, e.g., an imperfect material preparation process. We discuss, as an instance, disorders in offset refractive indices n_m which are simulated here by replacing n_m with $(1 + r_m)n_m$, being $r_m \in \{-r, r\}$ randomly generated numbers. We recalculate in Fig. 6 the diffraction patterns of Figs. 2, 4, and 5, yet in the presence of disorders and find that the missing diffraction orders start to appear for $r = 0.3$ in all three cases of directional elimination, grouped elimination, and directional selection. In other words, for our used parameters, rather steep (30%) random fluctuations in offset refractive indices are needed to observe the initial weak onset of all missing diffraction orders. We have further verified that, for lower disorder strengths, these rather dim diffraction peaks can be safely ignored (not shown), confirming the robustness of our grating against disorders in offset refractive indices and the validity of our results as compared to full-wave Comsol simulations.

IV. CONCLUSIONS

In summary, a pure phase grating has been designed to yield a spatially odd structure in terms of offset refractive indices for different elements in each period. It is of interest that this grating without loss and gain can produce highly asymmetric diffraction, which represents an uncommon way to break Friedel's law as it does not rely on an out-of-phase absorption modulation, but rather on multiple scattering processes. We have derived, in particular, three sufficient conditions on offset refractive indices for realizing the directional elimination of a single diffraction order, the grouped elimination of all even or odd diffraction orders, and the directional selection of a few diffraction orders, respectively. These intriguing phenomena are verified via numerical calculations and explained in terms of paired or sequential destructive interference between diffracted amplitudes contributed by the conjugate or adjacent elements in each period. Among them, selecting one or two diffraction orders on demand seems more appealing because it is beneficial in the development of high-precision signal-selecting optical devices.

We finally suggest that our main results might be implemented in recently flourishing metasurface platforms like in Refs. [42–44] where they could be further extended to the richer two-dimension case. Other materials with tunable refractive indices such as indium tin oxide [45] and germanium antimony tellurium alloy [46] might likewise be promising platforms where our asymmetric diffraction could be generated on demand.

ACKNOWLEDGMENTS

The work is supported by the National Natural Science Foundation of China (Grant No. 12074061), the Cooper-

ative Program by Italian Ministry of Foreign Affairs and International Cooperation (Grant No. PGR00960) and National Natural Science Foundation of China (Grant No. 11861131001), the Funding from Ministry of Science and Technology of China (Grant No. 2021YFE0193500), and the Joint Laboratories Program of the Italian Research Council (CNR) (Grant. No. SAC.AD002.026 (OMEN)). G.E.L. thanks the research project FSE-REACT EU financed by National Social Fund–National Operative Research Program and Innovation 2014–2020 (DM 1062/2021).

[1] C. Caucheteur, T. Guo, and J. Albert, Review of plasmonic fiber optic biochemical sensors: Improving the limit of detection, Anal. Bioanal. Chem. **407**, 3883 (2015).

[2] S. J. Mihailov, Fiber Bragg grating sensors for harsh environments, Sensors **12**, 1898 (2012).

[3] A. Zanutta, A. Bianco, M. Insausti, and F. Garzón, Volume phase holographic gratings for astronomy based on solid photopolymers, in *Advances in Optical and Mechanical Technologies for Telescopes and Instrumentation*, edited by R. Navarro, C. R. Cunningham, and A. A. Barto, International Society for Optics and Photonics Vol. 9151 (SPIE, Washington, D.C., 2014), pp. 1992–2006.

[4] L. H. J. Raijmakers, D. L. Danilov, R. A. Eichel, and P. H. L. Notten, A review on various temperature-indication methods for Li-ion batteries, Appl. Energy **240**, 918 (2019).

[5] M. S. Zubairy, A very brief history of light, in *Optics in Our Time*, edited by M. D. Al-Amri, M. M. El-Gomati, and M. S. Zubairy (Springer, Cham. 2016).

[6] M. Mitsunaga and N. Imoto, Observation of an electromagnetically induced grating in cold sodium atoms, Phys. Rev. A **59**, 4773 (1999).

[7] H. Y. Ling, Y.-Q. Li and M. Xiao, Electromagnetically induced grating: Homogeneously broadened medium, Phys. Rev. A **57**, 1338 (1998).

[8] J. T. Sheng, J. Wang, M. A. Miri, D. N. Christodoulides, and M. Xiao, Observation of discrete diffraction patterns in an optically induced lattice, Opt. Express **23**, 19777 (2015).

[9] J. P. Yuan, C. H. Wu, L. R. Wang, G. Chen, and S. T. Jia, Observation of diffraction pattern in two-dimensional optically induced atomic lattice, Opt. Lett. **44**, 4123 (2019).

[10] L. E. E. de Araujo, Electromagnetically induced phase grating, Opt. Lett. **35**, 977 (2010).

[11] S. A. de Carvalho and L. E. E. de Araujo, Electromagnetically induced phase grating: A coupled-wave theory analysis, Opt. Express **19**, 1936 (2011).

[12] N. Ba, L. Wang, X.-Y. Wu, X.-J. Liu, H.-H. Wang, C.-L. Cui, and A.-J. Li, Electromagnetically induced grating based on the giant Kerr nonlinearity controlled by spontaneously generated coherence, Appl. Opt. **52**, 4264 (2013).

[13] T. Naseri and R. Sadighi-Bonabi, Efficient electromagnetically induced phase grating via quantum interference in a four-level N-type atomic system, J. Opt. Soc. Am. B **31**, 2430 (2014).

[14] A. Vafafard and M. Mahmoudi, Switching from electromagnetically induced absorption grating to electromagnetically induced phase grating in a closed-loop atomic system, Appl. Opt. **54**, 10613 (2015).

[15] R. Sadighi-Bonabi, T. Naseri, and M. Navadeh-Toupchi, Electromagnetically induced grating in the microwave driven four-level atomic systems, Appl. Opt. **54**, 368 (2015).

[16] G. Friedel, Sur les symétries cristallines que peut révéler la diffraction des rayons Röntgen, C. R. Acad. Sci. (Paris) **157**, 1533 (1913).

[17] W. H. Zachariasen, *Theory of X-ray Diffraction in Crystals* (Wiley, New York, 1945).

[18] P. P. Ewald and C. Hermann, Gilt der Friedelsche Satz über die Symmetrie der Röntgeninterferenzen?, Z. Kristallogr. **65**, 251 (1927).

[19] S. Nishikawa and K. Matsukawa, Hemihedry of zincblende and x-ray reflexion, Proc. Imp. Acad. Japan **4**, 96 (1928).

[20] C. Keller, M. K. Oberthaler, R. Abfalterer, S. Bernet, J. Schmiedmayer, and A. Zeilinger, Tailored complex potentials and Friedel's Law in Atom Physics, Phys. Rev. Lett. **79**, 3327 (1997).

[21] M. V. Berry, Lop-sided diffraction by absorbing crystals, J. Phys. A: Math. Gen. **31**, 3493 (1998).

[22] X.-Y. Zhu, Y.-L. Xu, Y. Zou, X.-C. Sun, C. He, M.-H. Lu, X.-P. Liu, and Y.-F. Chen, Asymmetric diffraction based on a passive parity-time grating, Appl. Phys. Lett. **109**, 111101 (2016).

[23] Y.-M. Liu, F. Gao, C.-H. Fan, and J.-H. Wu, Asymmetric light diffraction of an atomic grating with PT symmetry, Opt. Lett. **42**, 4283 (2017).

[24] V. A. Bushuev, L. V. Dergacheva, and B. I. Mantsyzov, PT-symmetric photonic crystals under dynamical Bragg diffraction beyond the paraxial approximation, Phys. Rev. A **95**, 033843 (2017).

[25] Z. Y. Zhang, L. Yang, J. L. Feng, J. T. Sheng, Y. Q. Zhang, Y. P. Zhang, and M. Xiao, Parity-time-symmetric optical lattice with alternating gain and loss atomic configurations, Laser Photon. Rev. **12**, 1800155 (2018).

[26] T. Shui, W.-X. Yang, S. P. Liu, L. Li, and Z. H. Zhu, Asymmetric diffraction by atomic gratings with optical PT symmetry in the Raman-Nath regime, Phys. Rev. A **97**, 033819 (2018).

[27] D. D. Ma, D. M. Yu, X.-D. Zhao, and J. Qian, Unidirectional and controllable higher-order diffraction by a Rydberg electromagnetically induced grating, Phys. Rev. A **99**, 033826 (2019).

[28] Y.-M. Liu, F. Gao, J.-H. Wu, M. Artoni, and G. C. La Rocca, Lopsided diffractions of distinct symmetries in two-dimensional non-Hermitian optical gratings, Phys. Rev. A **100**, 043801 (2019).

[29] C. Hang, W. B. Li, and G. X. Huang, Nonlinear light diffraction by electromagnetically induced gratings with PT symmetry in a Rydberg atomic gas, Phys. Rev. A **100**, 043807 (2019).

[30] S. Miyake and R. Uyeda, An exception to Friedel's law in electron diffraction, Acta Cryst. **3**, 314 (1950).

[31] S. Miyake and R. Uyeda, Friedel's law in the dynamical theory of diffraction, Acta Cryst. **8**, 335 (1955).

[32] P. Deb, M. C. Cao, Y. Han, M. E. Holtz, S. Xie, J. Park, R. Hovden, and D. A. Muller, Imaging polarity in two dimensional materials by breaking Friedel's law, Ultramicroscopy **215**, 113019 (2020).

[33] M. W. Farn, M. B. Stern, W. B. Veldkamp, and S. S. Medeiros, Color separation by use of binary optics, Opt. Lett. **18**, 1214 (1993).

[34] J. B. Yang, X. Y. Su, and X. Ping, A module design of rearrangeable nonblocking double omega optical network using binary optics elements, Opt. Laser Technol. **40**, 756 (2008).

[35] C. Ma, X. H. Li, and N. X. Fang, Acoustic Angle-Selective Transmission Based on Binary Phase Gratings, Phys. Rev. Appl. **14**, 064058 (2020).

[36] M.-S. L. Lee, P. Lalanne, and J.-C. Rodier, Wide-field-angle behavior of blazed-binary gratings in the resonance domain, Opt. Lett. **25**, 1690 (2000).

[37] A. Vasara, J. Turunen, and A. T. Friberg, Realization of general nondiffracting beams with computer-generated holograms, J. Opt. Soc. Am. A **6**, 1748 (1989).

[38] I. A. Avrutsky, D. S. Ellis, A. Tager, H. Anis, and J. M. Xu, Design of widely tunable semiconductor lasers and the concept of binary superimposed gratings, IEEE J. Quantum Electron. **34**, 729 (1998).

[39] M. Khorasaninejad and F. Capasso, Metalenses: Versatile multifunctional photonic components, Science **358**, 1146 (2017).

[40] Z. M. Lin, X. W. Li, R. Z. Zhao, X. Song, Y. T. Wang, and L. L. Huang, High-efficiency Bessel beam array generation by Huygens metasurfaces, Nanophotonics **8**, 1079 (2019).

[41] A. V. Kildishev, A. Boltasseva, and V. M. Shalaev, Planar photonics with metasurfaces, Science **339**, 1232009 (2013).

[42] P. Genevet and F. Capasso, Holographic optical metasurfaces: A review of current progress, Rep. Prog. Phys. **78**, 024401 (2015).

[43] N. S. Nye, A. E. Halawany, C. Markos, M. Khajavikhan, and D. N. Christodoulides, Flexible PT-Symmetric Optical Metasurfaces, Phys. Rev. Appl. **13**, 064005 (2020).

[44] N. Yu and F. Capasso, Flat optics with designer metasurfaces, Nat. Mater. **13**, 139 (2014).

[45] Y.-W. Huang, H. W. H. Lee, R. Sokhoyan, R. A. Pala, K. Thyagarajan, S. Han, D. P. Tsai, and H. A. Atwater, Gate-tunable conducting oxide metasurfaces, Nano Lett. **16**, 5319 (2016).

[46] C. H. Chu, M. L. Tseng, J. Chen, P. C. Wu, Y.-H. Chen, H.-C. Wang, T.-Y. Chen, W. T. Hsieh, H. J. Wu, G. Sun and D. P. Tsai, Active dielectric metasurfaces based on phase-change medium, Laser Photon. Rev. **10**, 986 (2016).